

不同氧化程度的沥青纤维预氧化与炭化行为

彭元硕¹, 杨建校^{1,2}, 石奎¹, 郭建光¹, 朱辉², 李轩科^{1,2}

(1. 湖南大学 材料科学与工程学院, 先进炭材料及应用技术湖南省重点实验室, 湖南 长沙 410082;

2. 武汉科技大学, 煤转化与新型炭材料湖北省重点实验室, 湖北 武汉 430081)

摘要: 以各向同性沥青纤维(IPPF)和中间相沥青纤维(MPPF)为对象,系统研究了它们在不同升温速率和不同预氧化温度下的预氧化过程。通过元素分析,FT-IR, TG-MS 和 SEM 等手段对预氧化纤维(SFs)和碳纤维(CFs)进行了详细的分析表征,探究了沥青纤维的氧化程度对CFs的结构和力学性能的影响规律。结果表明,慢的升温速率有利于沥青纤维的氧化交联,所得到的CFs具有更高的炭化收率和拉伸强度。同时,IPPF和MPPF在270℃进行预氧化时,所制备对应的CFs具有最高的结构性能。另外,SFs的FT-IR图所计算的 R_{1700}/R_{1600} 值与其对应CFs的炭化收率和拉伸强度存在着良好的映射关系,可以作为一个评估沥青纤维的氧化程度的有效因子。除此之外,氧化不充足的纤维(I-SFs)在炭化过程中释放大量的 H_2 和 CH_4 ,造成所得到的CFs出现空心结构,显示低的拉伸强度,尤其I-IPCF较为明显;过度氧化的纤维(E-SFs)则释放大量的CO和 CO_2 ,导致其对应的CFs呈现裂缝结构,特别是E-MPCF。因此,纤维预氧化和炭化行为的深入解析与优化对于提升沥青基碳纤维的性能具有重大的意义。

关键词: 各向同性沥青;中间相沥青;沥青纤维;预氧化;碳纤维

中图分类号: TQ536.2

文献标识码: A

基金项目:国家自然科学基金青年项目(51702094);湖南省自然科学基金项目(2017JJ3014);煤转化与新型炭材料湖北省重点实验室2019年度开放基金资助项目(WKD201908)。

通讯作者:杨建校,助理教授。E-mail: yangjianxiao@hnu.edu.cn

作者简介:彭元硕。E-mail: 2317853120@qq.com

Effects of the degree of oxidation of pitch fibers on their stabilization and carbonization behaviors

PENG Yuan-shuo¹, YANG Jian-xiao^{1,2}, SHI Kui¹, GUO Jian-guang¹, ZHU Hui², LI Xuan-ke^{1,2}

(1. Hunan Province Key Laboratory for Advanced Carbon Materials and Applied Technology, College of Materials Science and Engineering,

Hunan University, Changsha 410082, China;

2. Key Laboratory of Hubei Province for Coal Conversion and New Carbon Materials,

Wuhan University of Science and Technology, Wuhan 430081, China)

Abstract: The stabilization of isotropic pitch-derived fibers (IPFs) and mesophase pitch-derived fibers (MPFs) in air was performed at different heating rates and with different final stabilization temperatures. The stabilized fibers (SFs) and carbon fibers (CFs) were characterized by elemental analysis, FT-IR, TG-MS and SEM to investigate the influence of the degree of oxidation of the SFs on the microstructures and mechanical properties of the CFs. Results showed that a slow heating rate during stabilization was beneficial to the oxidative cross-linking of PFs, and the corresponding CFs had a higher carbonization yield and tensile strength at the lower heating rate. When both IPF and MPF were stabilized at 270 °C, the two resulting CFs all reached their optimal performance. In addition, the FTIR peak intensity ratio of the C=O band at about 1700 cm^{-1} to the C=C band at 1600 cm^{-1} of the SFs had a good relationship to the carbonization yield and tensile strength of the CFs, and this can be used to optimize the degree of oxidation of the SFs. Moreover, insufficiently stabilized fibers released a great deal of H_2 and CH_4 , causing some porosity in the resulting CFs with a low tensile strength, especially for the insufficiently stabilized IPCF. While over-stabilized fibers released a large amount of CO and CO_2 , causing cracked textures in the corresponding CFs, especially in the over-stabilized MPCF. Therefore, this research into the stabilization and carbonization behaviors of pitch fibers has great significance for improving the mechanical properties of pitch-based CFs.

Key words: Isotropic pitch; Mesophase pitch; Pitch fibers; Stabilization; Carbon fibers

Received date: 2019-08-07; *Revised date:* 2019-10-11

Foundation item: National Natural Science Foundation for Young Scientists of China (51702094), Natural Science Foundation for Young Scientists of Hunan Province (2017JJ3014), Key Laboratory of Hubei Province for Coal Conversion and

New Carbon Materials (WKD201908).

Corresponding author: YANG Jian-xiao, Assistant professor. E-mail: yangjianxiao@hnu.edu.cn

Author introduction: PENG Yuan-shuo Doctor student. E-mail: 2317853120@qq.com

1 Introduction

Pitch-based carbon fibers (CFs) were manufactured through a series of processes, including preparation of pitch precursors, spinning, stabilization, carbonization and graphitization^[1-3]. Among these processes, the stabilization played an important role in ensuring the infusibility of pitch fibers (PFs) before carbonization, which was vital to improve the carbonization yield and mechanical properties of CFs^[4-7]. A number of literatures indicated that some significant physical and chemical changes of PFs would occur during the stabilization. In general, the stabilization could form oxygen bridge structures through oxidation, dehydrogenation and cross-linking of pitch molecules, which prevented PFs from melting during carbonization^[8,9]. Moreover, the oxidation degree of stabilized fibers (SFs) was also a determining factor on the performance of the corresponding CFs. Insufficient stabilization might cause some problems such as melting and uneven shrinkage of fibers during carbonization. While excess stabilization might bring about the formation of defects by decomposition of oxidized molecules and of the lowered carbonization yield^[10,11]. However, the chemical and physical changes of PFs were complex and difficult to be described during stabilization because of the complexity of pitch precursors. In recent years, Yoon et al^[12] developed a simple mean to monitor and optimize the stabilization parameters of mesophase pitch fibers by thermal analyses at several heating rates, and discovered that a lower heating rate gave rise to a larger maximum weight gain by a more oxygen uptake. Zhu et al^[13] observed the evolution of chemical structure and released gases in stabilization of isotropic pitch fibers by FT-IR and MS and obtained the optimal stabilization temperature and time in stabilization. Moreover, Jang et al^[14] measured the densities of SFs with different stabilization conditions which could be used as a reasonable index to evaluate the oxidation degree of SFs for producing high-performance CFs. Based on the research achievements of these scholars on the stabilization mechanisms of PFs, we should further investigate the differences of stabilization and carbonization behaviors of fibers with different oxidation degrees for optimizing the structure and properties of the pitch-based CFs. In fact, the weight gain of PFs due to oxygen uptake was dominant compared with the removal of

low molecular weight components in the PFs during stabilization^[14]. Meanwhile, the gas amounts released of SFs with different oxidation degrees were different during carbonization and had a great impact on the properties of the resultant CFs^[10]. Therefore, in this study, we analyzed a series of SFs with different stabilization conditions and the corresponding CFs in order to further understand the stabilization and carbonization behaviors of PFs. It is aimed to build up a correlation between the stabilization conditions of PFs or the properties of SFs and the structural or mechanical properties of the corresponding CFs.

2 Experimental

2.1 Materials

The ethylene tar was used as a raw material for preparing the spinnable pitch, which was supplied by Wuhan Luhua Yueda Chemical Co. Ltd., China. The ethylene tar-derived isotropic pitch (IP) was prepared by the atmospheric distillation at 380 °C for 5 h^[15], while the ethylene tar-derived mesophase pitch (MP) was prepared by a two-stage heat treatment, which consisted of the firstly pressurized treatment at 420 °C for 2 h and the successive atmospheric purging treatment at 410 °C for 2 h^[16]. The obtained IP and MP were melt-spun into pitch fibers (PFs) at the spinning temperature 80 °C higher than their softening points (SP) with a single-hole spinneret. The diameters of the resulting IP-derived PFs (IPPFs) and MP-derived PFs (MPPFs) were about 12 and 14 μm, respectively.

2.2 Stabilization and carbonization of pitch fibers

The IPPFs and MPPFs were stabilized in a corundum tube furnace under a 200 mL · min⁻¹ air flow with different heating rates (0.5, 1, 2, 4 °C · min⁻¹) from room temperature to the different stabilization temperature (230-370 °C) for 1 h. Then, the obtained stabilized fibers (SFs) were successively carbonized in a corundum tube furnace under a 200 mL · min⁻¹ nitrogen flow with a heating rate of 5 °C · min⁻¹ from room temperature to 1 000 °C for 10 min. The resulting SFs and CFs were labeled as IPSF-X-Y, MPSF-X-Y, IPCF-X-Y and MPCF-X-Y, respectively. Where X and Y represented the stabilization temperature and the heating rate during stabilization.

2.3 Characterization of pitches and fibers

The SPs and optical texture of pitches were de-

terminated by a CFT-100EX capillary rheometer (Shimadzu) and a BX53 polarizing microscope (POM, Olympus), respectively. The oxygen contents of pitches and fibers were determined by a Vario EL III elemental analyzer (Elementar) with the subtracting method ($O = 100 - C - H - N - S$). The functional groups of pitches and fibers were analyzed by a Nicolet iS10 Fourier transform infrared spectrometer (FT-IR, Thermo Fisher Scientific). The thermal stability of pitches was measured using a STA 449 F5 thermogravimetric analyzer (TG, Netzsch) under a $40 \text{ mL} \cdot \text{min}^{-1}$ nitrogen flow with a heating rate of $5 \text{ }^\circ\text{C} \cdot \text{min}^{-1}$ to $1\ 000 \text{ }^\circ\text{C}$. Meanwhile, to evaluate the stabilization properties of PFs, the obtained PFs were also analyzed by a TG analyzer with different heating rates ($0.5, 1, 2, 4 \text{ }^\circ\text{C} \cdot \text{min}^{-1}$) to $600 \text{ }^\circ\text{C}$ in a $40 \text{ mL} \cdot \text{min}^{-1}$ air flow to find their maximum weight gain (W_{max}) and the corresponding temperature (T) as well as to calculate their reaction activation energy (E_a) through the Kissinger's method^[17]. The morphologies and diameters of CFs were observed by a JSM-6700F field emission scanning electron microscope (SEM, JEOL) with 5 kV . The tensile strength of CFs was measured at room temperature using monofilaments with a gauge length of 20 mm according to the standard (ASTM D4018-2011) from the mean value of 30 tests with the values distributing within 10%. Finally, the released gases of SFs with different oxidation degrees were measured by a Hiden Analytical HAS-301-1474 mass spectrometer (MS, Hiden Analytical) coupled with TG, which was heated from room temperature to $1\ 400 \text{ }^\circ\text{C}$ with a heating rate of $10 \text{ }^\circ\text{C} \cdot \text{min}^{-1}$ under a $20 \text{ mL} \cdot \text{min}^{-1}$ argon flow. The MS was performed at the RGA mode with a secondary electron multiplier, and the quartz capillary connected to the thermal analyzer was heated to $160 \text{ }^\circ\text{C}$.

3 Results and discussion

3.1 Characterization of pitch precursors and their pitch fibers

The general properties of IP and MP were summarized in Table 1. The yield of IP and MP was 23% and 15%, respectively. The MP contained a slightly higher oxygen content of 0.99% and lower hydrogen

content of 3.86% than those of IP of 0.40% and 4.98%, respectively. The POM photos of IP and MP are shown in Fig. 1(a) and (b), respectively. The IP showed an evident isotropic feature, while the MP had a wide-area streamline feature with a mesophase content over 90% due to the stacking of its planar macromolecules. The rheological curves of IP and MP were measured by a capillary rheometer as shown in Fig. 1(c), which indicated that the SPs of IP and MP were about 255 and 275 $^\circ\text{C}$, respectively (Table 1). Moreover, the TG curves of IP and MP in the nitrogen atmosphere are shown in Fig. 1(d). The results showed that the MP had a higher decomposition temperature than that of IP due to the higher polymerization degree of MP, in accordance with the higher SP of MP, and the coking value of MP was much higher than that of IP. The results also could be attributed to the fact that MP had a higher aromatic degree and average molecular weight than IP^[15, 18]. Therefore, these differences in the molecular structures of pitch precursors would affect spinning, stabilization and carbonization behaviors as well as the structures and properties of the resultant CFs.

On the other hand, the oxidative abilities of IPPF and MPPF were investigated by TGA under air atmosphere with different heating rates of 0.5, 1, 2 and 4 $^\circ\text{C} \cdot \text{min}^{-1}$ as shown in Fig. 2. The weight gain of both IPPF and MPPF decreased with the heating rate and the decomposition temperature of both IPPF and MPPF increased with the heating rate. However, the initial temperature of weight gain of IPPF was about $180 \text{ }^\circ\text{C}$, which was lower than that of MPPF about $200 \text{ }^\circ\text{C}$ due to the fact that IPPF consisted of more aliphatic groups than MPPF. And the maximum weight gain of IPPF was much higher than that of MPPF due to the higher oxidative ability of IP precursor, which was supported by the fact that E_a of IP and MP was 121 and 91 $\text{kJ} \cdot \text{min}^{-1}$, respectively (Table 1). Therefore, MPPF with a higher aromatic degree and higher molecular showed a better thermal stability, but lower oxidative ability than IPPF. And these results indicated that IPPF and MPPF would have different stabilization behaviors due to the differences in pitch molecular structures and their oxidative abilities.

Table 1 Elemental contents, softening point and activation energy of IP and MP precursors.

Sample	Yield(%)	SP($^\circ\text{C}$)	C(%)	H(%)	N(%)	S(%)	O(%)	$E_a(\text{KJ} \cdot \text{mol}^{-1})$
IP	23	255	94.53	4.98	0.04	0.05	0.40	121
MP	15	275	95.07	3.86	0.04	0.04	0.99	97

3.2 Characterization of stabilized fibers and carbon fibers

3.2.1 Stabilization with different heating rates

Fig. 3 shows the stabilization and carbonization yields of fibers, and the tensile strength of CFs at different heating rates in stabilization. The stabilization and carbonization yields of fibers, as well as the tensile strength of CFs decreased with increasing the

heating rate from 0.5 to 4 °C · min⁻¹. Meanwhile, the MP-derived fibers showed a lower stabilization yield and higher carbonization yield than those of IP-derived fibers. Moreover, the MPCF possessed a higher tensile strength than the IPCF, and the maximum tensile strength of IPCF and MPCF carbonized at 1 000 °C reached 630 and 1 019 MPa, respectively.

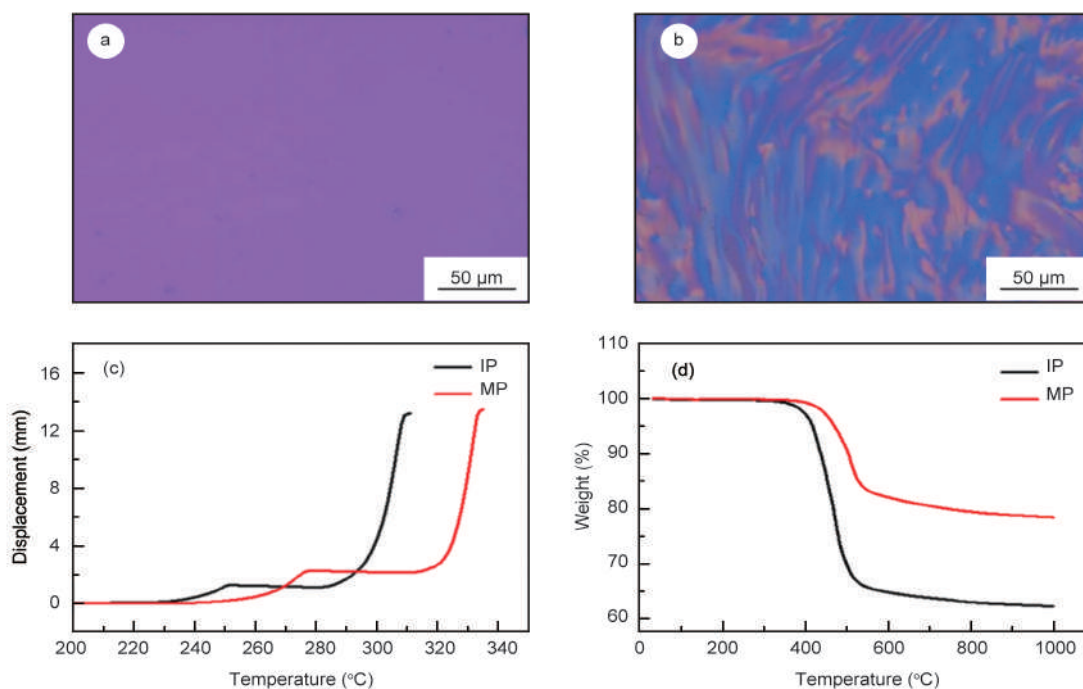


Fig. 1 POM photos of (a) IP, (b) MP precursors, (c) rheological curves and (d) TG curves of IP and MP precursors.

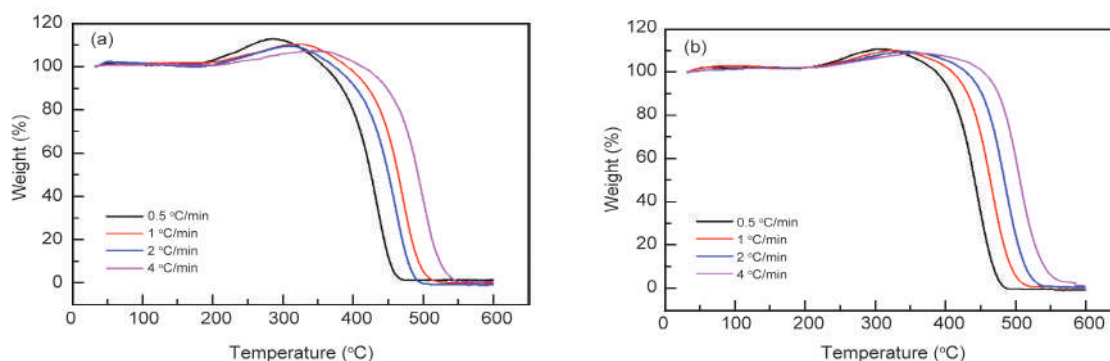


Fig. 2 TG curves of (a) IPPFs and (b) MPPFs from room temperature to 600 °C with heating rates of 0.5, 1, 2 and 4 °C · min⁻¹ under air atmosphere.

In order to investigate the chemical structural evolution of two different PFs after stabilization, the FT-IR spectra of their PFs and SFs with different heating rates are shown in Fig. 4 (a) and (b). For two as-spun PFs, the aliphatic C—H bending, aromatic C=C stretching, aliphatic C—H stretching and aromatic C—H stretching peaks were observed at 1 460, 1 600, 2 960, and 3 050 cm⁻¹, respectively, and some peaks in the region 700-900 cm⁻¹ corre-

sponded to the out-of-plane C—H and ring bends. As to the obtained SFs, the stabilization led to the appearance of new peaks at 1 260 and 1 700 cm⁻¹ corresponding to C—O—C or O—C—O stretching and carbonyl C=O stretching, respectively, indicating the existence of ketone, carboxylate, and carbonate groups in the SFs. Moreover, the intensities of peaks at 750, 1 460, 2 960 and 3 050 cm⁻¹ obviously decreased with the heating rate. In order to clearly eval-

uate the oxidation degree of SFs, the peak intensity ratio of the C=O band at about 1700 cm^{-1} (R_{1700}) to the C=C band at 1600 cm^{-1} (R_{1600}) was calculated from FT-IR as shown in Fig. 7^[14, 19]. It could be seen from Fig. 7(a) that R_{1700}/R_{1600} gradually decreased with increasing the heating rate from 0.5 to $4\text{ }^{\circ}\text{C}\cdot\text{min}^{-1}$ for both of IPSF and MPSF. It indicated that the stabilization of PFs was more complete at a lower heating rate, and the corresponding CFs also exhibited a higher tensile strength and carbonization yield. In addition, the R_{1700}/R_{1600} of IPSF was higher than that of MPSF, and it was also suggested that MPPF was more difficult to be oxidized than IPPF.

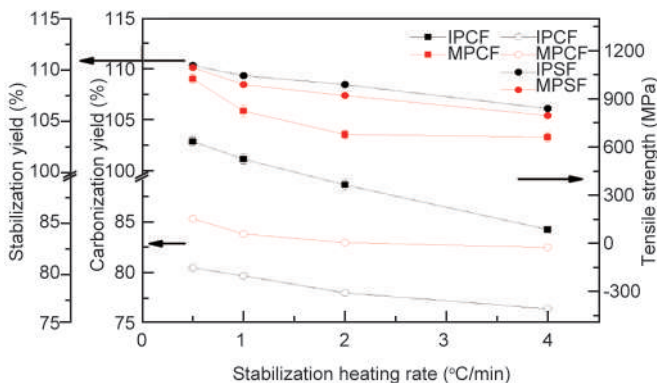
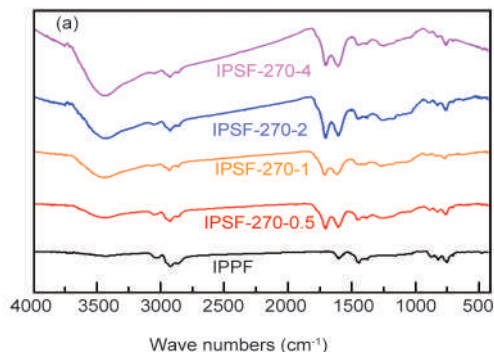


Fig. 3 The stabilization yield of SFs and the carbonization yield and tensile strength of CFs as a function of stabilization heating rates.

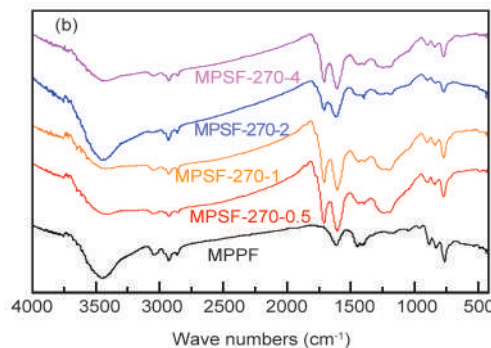


Fig. 4 FT-IR spectra of (a) IPSFs and (b) MPSFs prepared with different heating rates of $0.5, 1, 2$ and $4\text{ }^{\circ}\text{C}\cdot\text{min}^{-1}$.

3.2.2 Stabilization with different target temperatures

Fig. 5 shows the stabilization and carbonization yields of fibers, and the tensile strength of CFs obtained at different target temperatures in stabilization. The stabilization yield of fibers increased with increasing the stabilization temperature, but decreased when the stabilization temperature was over $330\text{ }^{\circ}\text{C}$. Otherwise, the carbonization yield and tensile strength of CFs presented their maximum values (carbonization yield: 80.6% for IPCF, 85.5% for MPCF, and tensile strength: 520 MPa for IPCF, 820 MPa for MPCF) at a stabilization temperature of $270\text{ }^{\circ}\text{C}$. These results indicated that the higher weight gain of SFs was not conducive to achieve the more excellent properties of the resultant CFs. Therefore, the suitable stabilization temperature should be selected below the corresponding temperature of the maximum weight gain in the TG curves of SFs^[20].

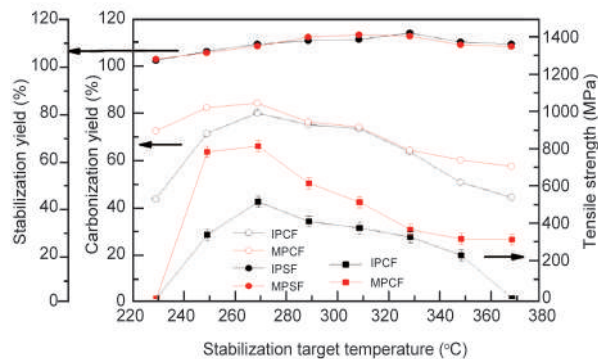


Fig. 5 The stabilization yield of SFs and the carbonization yield and tensile strength of CFs as a function of stabilization target temperatures.

Fig. 6 shows the FT-IR spectra of two different PFs and their SFs with different heat treatment temperatures in stabilization. Obviously, when the stabilization temperature was $230\text{ }^{\circ}\text{C}$, the peaks at around 1260 and 1700 cm^{-1} were very weak. It indicated that a small amount of C=O, C—O—C and O—C—O bonds appeared. Along with the rise of temperature, the peak at around 1700 cm^{-1} increased. Besides

this, when the temperature was above $330\text{ }^{\circ}\text{C}$, the peaks at around 1260 cm^{-1} gradually increased and the peaks at 2960 and 3050 cm^{-1} were gradually weakened. And more distinct peaks were observed at 1260 cm^{-1} , indicating that more oxygen introduced more C—O oxygen-functional groups^[13]. Otherwise, it could be seen from Fig. 7(b) that the maximum of R_{1700}/R_{1600} appeared at $270\text{ }^{\circ}\text{C}$, and the corresponding CFs showed the highest carbonization yield and tensile strength. Therefore, the R_{1700}/R_{1600} could be used as a factor to evaluate the suitable stabilization conditions because there was a good relationship between the R_{1700}/R_{1600} of SFs and the tensile strength of CFs.

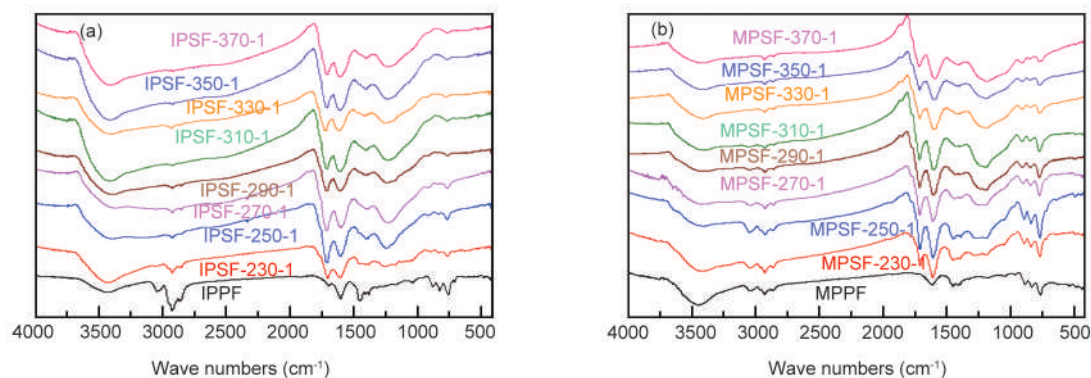


Fig. 6 FT-IR spectra of (a) IPSFs and (b) MPSFs prepared with different stabilization target temperatures of 230 to 370 °C.

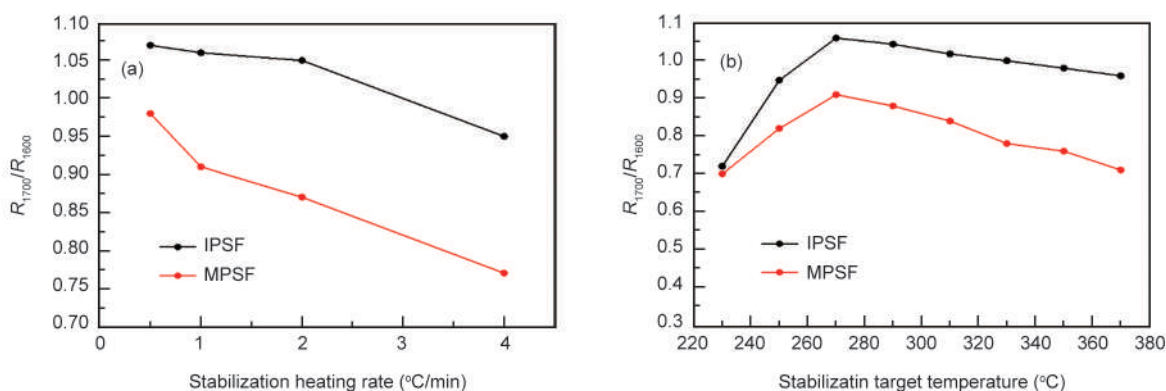


Fig. 7 R_{1700}/R_{1600} of IPSFs and MPSFs (a) prepared with different heating rates and (b) prepared with different stabilization target temperatures.

3.3 Exploring the carbonization behaviors of stabilized fibers with different oxidation degrees

According to the above experimental results, three typical SFs with different oxidation degrees were selected to explore their carbonization behaviors. The information of selected SFs were as follows; IPSF-270-4 and MPSF-270-4 were selected as the insufficient stabilized fibers (I-SFs), IPSF-330-1 and MPSF-330-1 were selected as the excess stabilized fibers (E-SFs) and IPSF-270-0.5 and MPSF-270-0.5 were selected as the normal stabilized fibers (N-SFs). Table 2 summarizes the stabilization yield, carbonization yield, elemental contents, diameter and tensile strength of their SFs and CFs. It was noticed that E-SFs showed a highest stabilization yield among E-SFs, I-SFs and N-SFs, which was in accordance with the much highest introduced oxygen content in the E-SFs (31.92% for E-IPSF, 21.82% for E-MPSF). While the E-CFs showed a lowest carbonization yield (50.1% for E-IPCF, 63.9% for E-MPCF), caused by the release of more oxygen-containing gases during carbonization. Thus, the E-CFs might have many defects in the carbonized fibers, re-

sulting in its lowest tensile strength (232 MPa for E-IPCF with diameter of about 10.98 μm , 370 MPa for E-MPCF with diameter of about 13.02 μm) of the resultant CFs. On the other hand, the I-CFs also showed the lower tensile strength (83 MPa for I-IPCF with diameter of about 11.80 μm , 466 MPa for I-MPCF with diameter of about 13.87 μm) than the N-CFs due to their insufficient oxidation, which might lead to the skin-core structure of the resultant CFs. These assumptions would be supported by the following analyses of TG-MS and SEM results.

As shown in Fig. 8, the TG curves of SFs showed that E-SFs were intensively decomposed from 400 °C and had much a lower carbonization yield at a higher temperature in comparison with the corresponding I-SFs and N-SFs. It was because that E-SFs released a large amount of gases in the late stage of carbonization due to their high oxygen contents (Table 2). Moreover, MPSF showed a higher carbonization yield at 1000 °C than IPSF due to their differences in the pitch precursor compositions.

The MS curves about the evolution of H_2 , CH_4 , CO and CO_2 of I/N/E-IPSF and I/N/E-MPSF during

Table 2 General properties of IPSFs and MPSFs with different oxidative degrees, and their resultant IPCFs and MPCFs.

Sample	Yield (%)	C (%)	H (%)	N (%)	S (%)	O (%)	D (μm)	TS (MPa)
I-IPSF	106.0	83.30	3.88	0.09	0.03	12.70	12.23	—
N-IPSF	110.3	79.09	3.37	0.10	0.03	17.41	12.51	—
E-IPSF	114.1	65.31	2.56	0.16	0.05	31.92	12.73	—
I-MPSF	105.3	85.78	3.28	0.08	0.05	10.81	14.13	—
N-MPSF	110.1	83.82	3.15	0.08	0.02	12.93	14.43	—
E-MPSF	12.7	75.57	2.52	0.06	0.03	21.82	14.78	—
I-IPCF	76.5	88.70	1.29	0.12	0.07	9.82	11.80	83
N-IPCF	80.6	85.11	3.97	0.13	0.01	10.78	11.56	630
E-IPCF	50.1	82.58	3.97	0.12	0.04	13.29	10.98	232
I-MPCF	82.6	94.16	0.94	0.08	0.04	4.78	13.87	466
N-MPCF	85.5	95.23	0.73	0.07	0.02	3.95	13.11	1019
E-MPCF	63.9	92.73	0.71	0.10	0.03	6.43	13.02	370

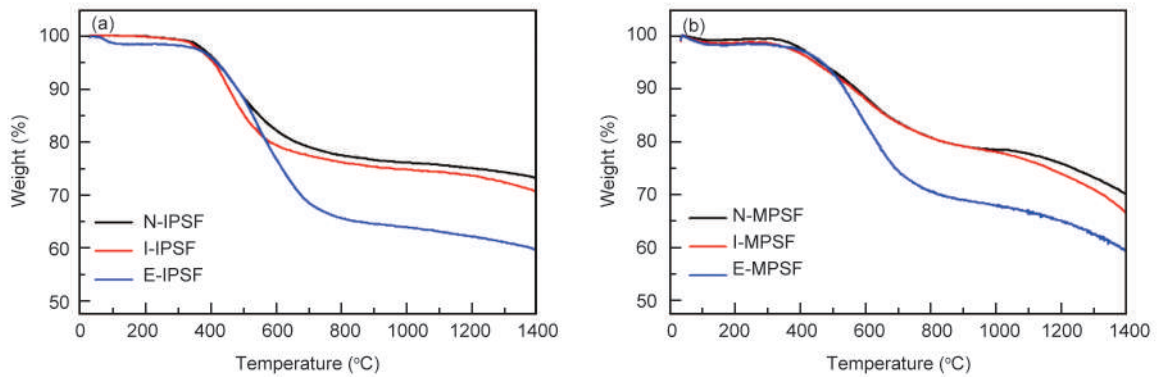


Fig. 8 TG curves of (a) N/I/E-IPSF and (b) I/N/E-MPSF from room temperature to 1 400 °C with a heating rate of 10 °C · min⁻¹ under argon atmosphere.

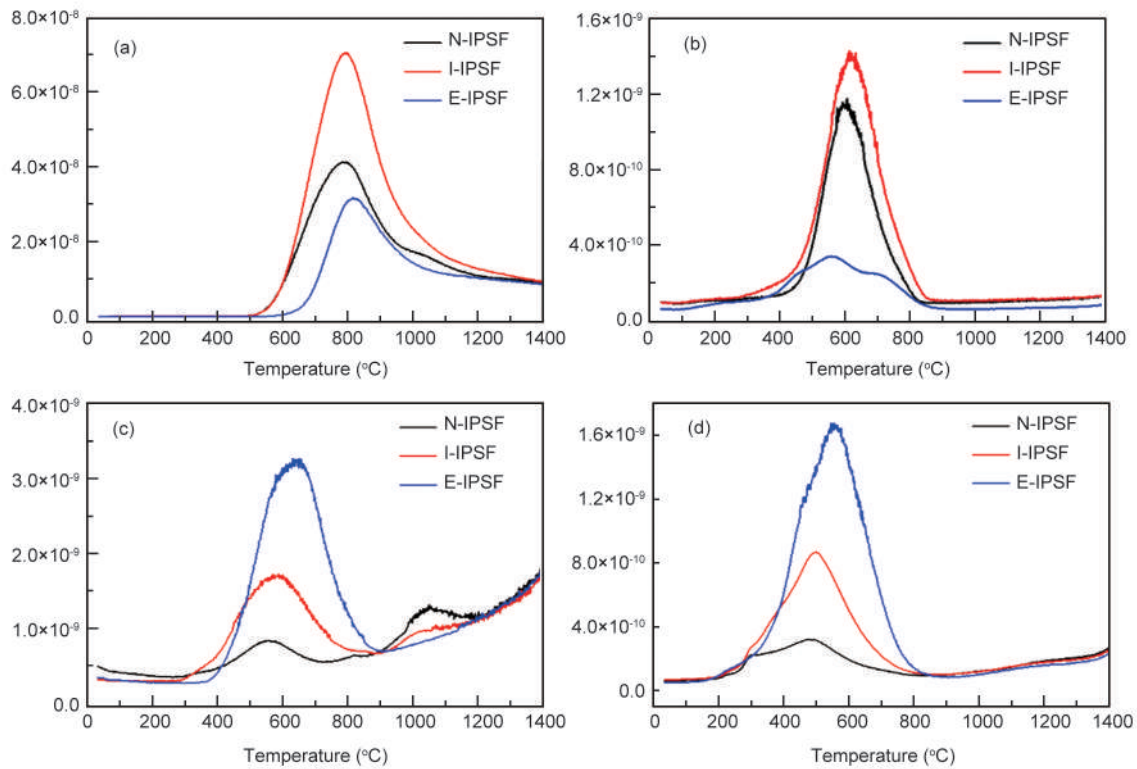


Fig. 9 The concentration changes of (a) H₂, (b) CH₄, (c) CO and (d) CO₂ of I/N/E-IPSF from room temperature to 1 400 °C with a heating rate of 10 °C · min⁻¹ under argon atmosphere.

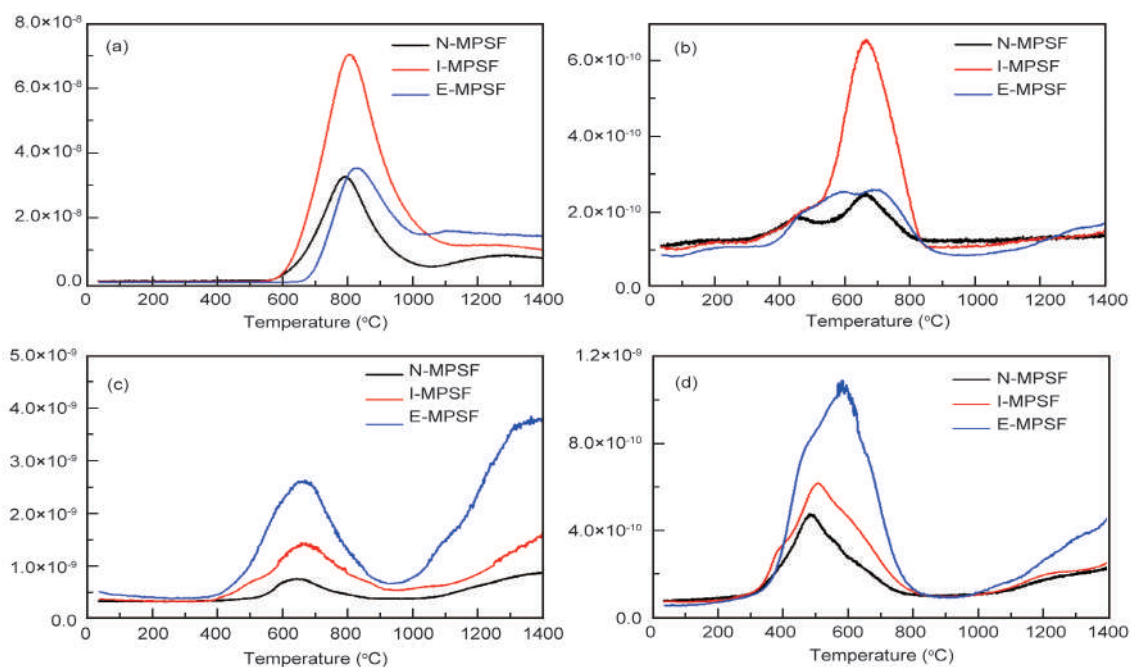


Fig. 10 The concentration changes of (a) H_2 , (b) CH_4 , (c) CO and (d) CO_2 of I/N/E-MPSF from room temperature to 1 400 °C with a heating rate of $10\text{ }^\circ\text{C} \cdot \text{min}^{-1}$ under argon atmosphere.

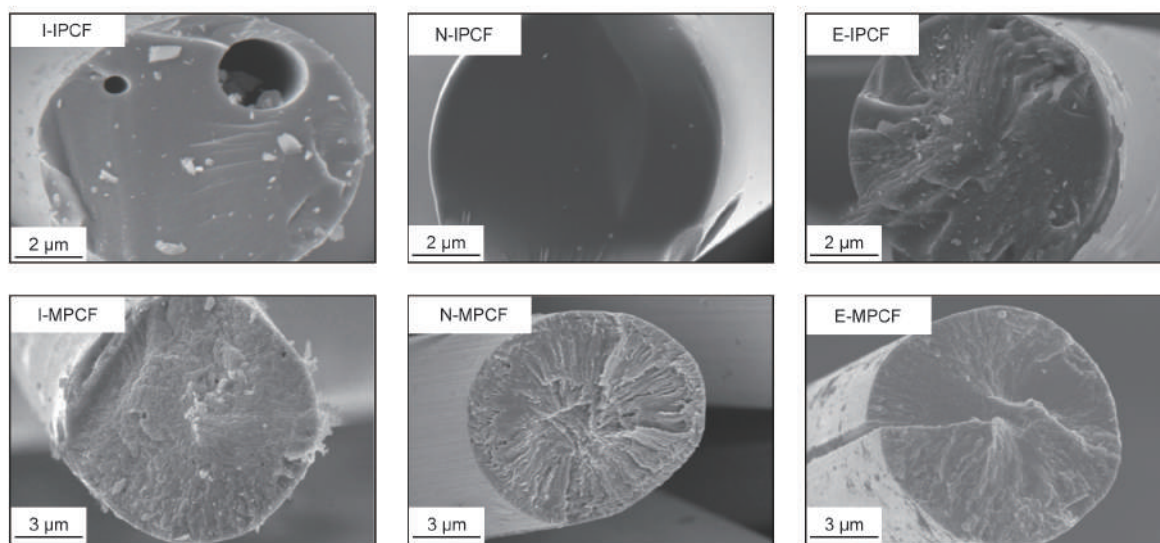


Fig. 11 Cross-section SEM images of CFs prepared from SFs with different oxidative degrees.

their carbonization are shown in Fig. 9 and Fig. 10. The H_2 started to produce above 500 °C, and the maximum values were found at about 800 °C for both of IPSF and MPSF. The evolution of CH_4 began at 400 °C, and the maximal peak values were observed at about 600 and 650 °C for IPSF and MPSF, respectively, which represented the decomposition of aliphatic compounds. It could be observed that the amounts of H_2 and CH_4 released from I-SFs were rather higher compared with N-SFs and E-SFs for both of IPSF and MPSF. This result could be explained that insufficient

stabilization was difficult to form stable cross-linked structure in the core of fibers, causing that more H was removed at the early stage of carbonization due to the deoxygenation^[21]. The CO was derived from the acid anhydrides that were developed by oxidation, and the maximal peak values of CO were observed at about 600 and 670 °C, for IPSF and MPSF, respectively. The evolution of CO_2 behaved the similar trend as CO , but the maximal peak values of CO_2 appeared at 500-600 °C, corresponding to the decomposition of carboxyl groups. It was evident that the a-

mounts of CO and CO₂ released from E-SFs were the highest among E-SFs, I-SFs and N-SFs due to the largest amounts of the oxygen-containing functional groups of E-SFs. It was due to the fact that E-SFs showed the highest oxygen contents from Table 2 (31.92% for E-IPSF, 21.82% for E-MPSF). In addition, the N-SFs released the lower amount of CO and CO₂ than I-SFs even N-SFs consisting the higher oxygen content, which indicated that the formed oxygen-functional groups of N-SFs were more stable than those of I-SFs. Fig. 11 shows the cross-section SEM images of CFs prepared from SFs with different oxidation degrees. It could be observed that I-IPCF and I-MPCF appeared the hollow structure and pore structure, respectively. While the cross-section of E-IPCF and E-MPCF appeared different levels of pore structure and cracked structure, respectively. These defects were consistent with the above MS analysis. Meanwhile, the resultant I-CFs and E-CFs had poor mechanical properties. Therefore, SFs had different oxidation degrees, and the corresponding CFs exhibited different structures and mechanical properties due to the differences in the amount of gases released of SFs during carbonization.

4 Conclusions

Ethylene tar-derived IPPF and MPPF were stabilized with different heating rates and stabilization temperatures. Research found that oxidative cross-linking of PFs was easier to conduct at a lower heating rate, and the obtained CFs possessed a higher carbonization yield and tensile strength. Otherwise, a suitable stabilization temperature was beneficial to the preparation of high-performance CFs. In addition, I-SFs released a more amount of H₂ and CH₄ while E-SFs released a more amount of CO and CO₂ during carbonization compared with N-SFs. As a result, the resultant I-CFs and E-CFs appeared the hollow and pore structure or cracked structure in the fibers, showing poorer mechanical properties. Accordingly, the PFs should be stabilized at a low heating rate and suitable stabilization temperature for the performance optimization of pitch-based CFs.

References

- [1] Frank E, Stuedle L M, Ingildeev D, et al. Carbon fibers: Precursor systems, processing, structure, and properties [J]. *Angewandte Chemie International Edition*, 2014, 53: 5262-5298.
- [2] FAN Zhen, Cao Min, YANG Wen-bin, et al. The evolution of microstructure and thermal conductivity of mesophase pitch-based carbon fibers with heat treatment temperature [J]. *New Carbon Materials*, 2019, 34(1): 38-43.
- [3] Liu J, Shimanoe H, Nakabayashi K, et al. Enhancing the oxidative stabilization of isotropic pitch precursors prepared through the co-carbonization of ethylene bottom oil and polyvinyl chloride [J]. *Journal of Industrial and Engineering Chemistry*, 2018, 67: 358-364.
- [4] SHI Jing-li, MA Chang. Preparation and characterization of spinnable mesophase pitches: A review [J]. *New Carbon Materials*, 2019, 34(3): 211-219.
- [5] Wang Y G, Chang Y C, Ishida S, et al. Stabilization and carbonization properties of mesocarbon microbeads (MCMB) prepared from a synthetic naphthalene isotropic pitch [J]. *Carbon*, 1999, 37: 969-976.
- [6] Lee T, Ooi C H, Othman R, et al. Activated carbon fiber – the hybrid of carbon fiber and activated carbon [J]. *Reviews on Advanced Materials Science*, 2014, 36: 118-136.
- [7] Rahaman M S A, Ismail A F, Mustafa A. A review of heat treatment on polyacrylonitrile fiber [J]. *Polymer Degradation and Stability*, 2007, 92: 1421-1432.
- [8] Drbohlav J, Stevenson W T K. The oxidative stabilization and carbonization of a synthetic mesophase pitch, part I: The oxidative stabilization process [J]. *Carbon*, 1995, 33: 693-711.
- [9] Zhu J, Park S W, Joh H I, et al. Preparation and characterization of isotropic pitch-based carbon fiber [J]. *Carbon Letters*, 2013, 14: 94-98.
- [10] Lim T H, Yeo S Y. Investigation of the degradation of pitch-based carbon fibers properties upon insufficient or excess thermal treatment [J]. *Scientific Reports*, 2017, 7: 4733.
- [11] Matsumoto T, Mochida I. Oxygen distribution in oxidatively stabilized mesophase pitch fiber [J]. *Carbon*, 1993, 31: 143-147.
- [12] Yoon S H, Korai Y, Mochida I. Assessment and optimization of the stabilization process of mesophase pitch fibers by thermal analyses [J]. *Carbon*, 1994, 32: 281-287.
- [13] Zhu J, Park S W, Joh H I, et al. Study on the stabilization of isotropic pitch based fibers [J]. *Macromolecular Research*, 2015, 23: 79-85.
- [14] Jang S Y, Ko S, Jeon Y P, et al. Evaluating the stabilization of isotropic pitch fibers for optimal tensile properties of carbon fibers [J]. *Journal of Industrial and Engineering Chemistry*, 2017, 45: 316-322.
- [15] Shi K, Yang J, Ye C, et al. A Comparison of ethylene-tar-derived isotropic pitches prepared by air blowing and nitrogen distillation methods and their carbon fibers [J]. *Materials*, 2019, 12: 305.
- [16] Shi K, Zhang X, Wu W, et al. Effect of the oxygen content and the functionality of spinnable pitches derived from ethylene tar by distillation on the mechanical properties of carbon fibers [J]. *New Carbon Materials*, 2019, 34: 84-94.
- [17] Régnier N, Fontaine S. Determination of the thermal degradation kinetic parameters of carbon fibre reinforced epoxy using TG [J]. *Journal of Thermal Analysis and Calorimetry*, 2001, 64: 789-799.
- [18] Yuan G, Jin Z, Zuo X, et al. Effect of carbonaceous precursors on the structure of mesophase pitches and their derived cokes [J]. *Energy & Fuels*, 2018, 32(8): 8329-8339.
- [19] Liu D, Ouyang Q, Jiang X, et al. Thermal properties and thermal stabilization of lignosulfonate-acrylonitrile-itaconic acid terpolymer for preparation of carbon fiber [J]. *Polymer degradation and stability*, 2018, 150: 57-66.
- [20] Kil H S, Jang S Y, Ko S, et al. Effects of stabilization variables on mechanical properties of isotropic pitch based carbon fibers [J]. *Journal of Industrial and Engineering Chemistry*, 2018, 58: 349-356.
- [21] Kil H S, Oh K, Kim Y J, et al. Structural evolution of pitch fibers during low temperature carbonization [J]. *Journal of Analytical and Applied Pyrolysis*, 2018, 136: 153-159.